Oxidation and Microstructural Evolution: Computational Investigations & Model Development

You-Hai Wen

Tianle Cheng, Jeffrey Hawk, and David Alman

US Department of Energy – NETL Albany, OR 97321, USA

Mar 21, 2017

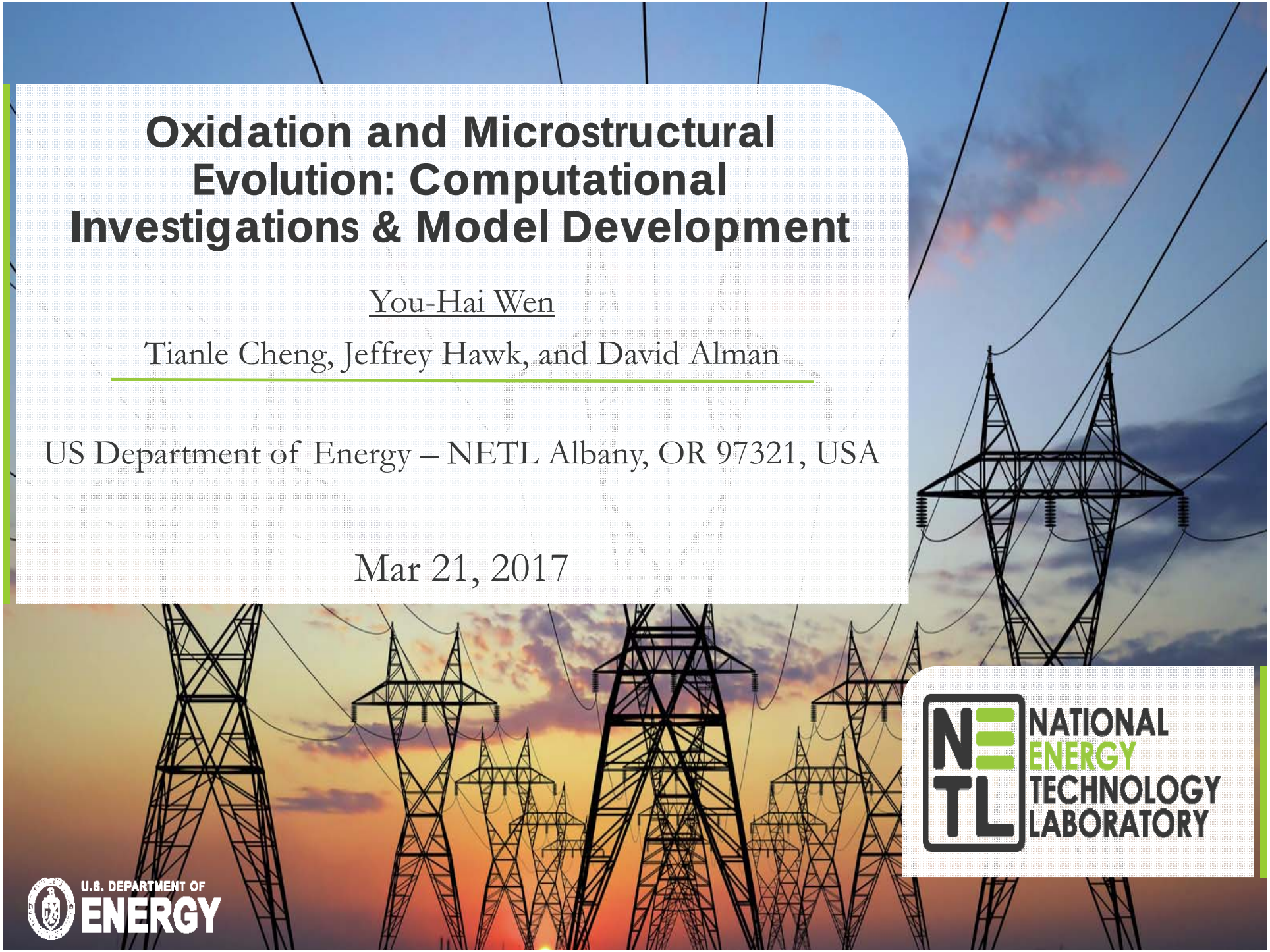

This work was funded by the Crosscutting Technologies Program at the National Energy Technology Laboratory (NETL) – managed by Robert Romanosky (Technology Manager). The Research was executed through NETL's Research and Innovation Center's Advanced Alloy Development Field Work Proposal.

NETL Engaged in Research at Developing Strategies to Mitigate Materials Degradation under Harsh Service Conditions

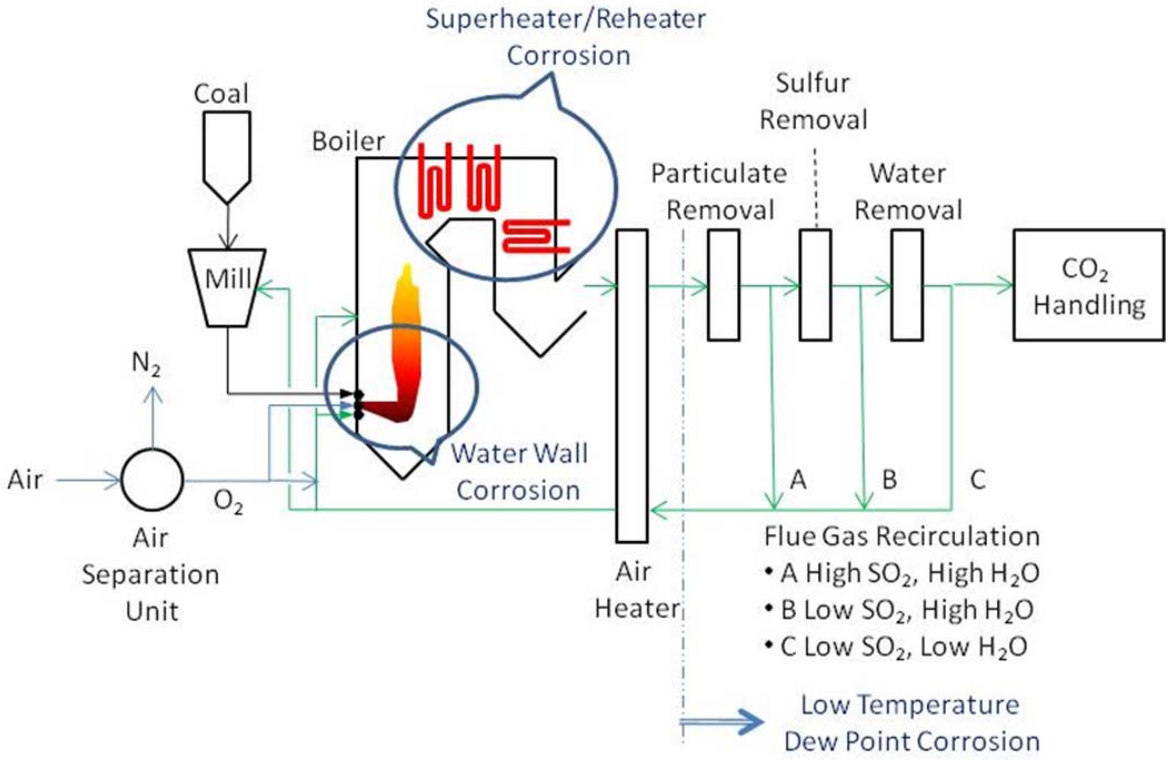

Advanced FE systems

- Environment is corrosive, high temperature, and high pressure
- Components have to last up to 300,000 hours

➢ ***Lack of experience with alloy performance in these conditions***

An integral computational and experimental approach to mitigate materials degradation

Microstructural Evolution

Subgrain, precipitate, and dislocation structure

As-tempered

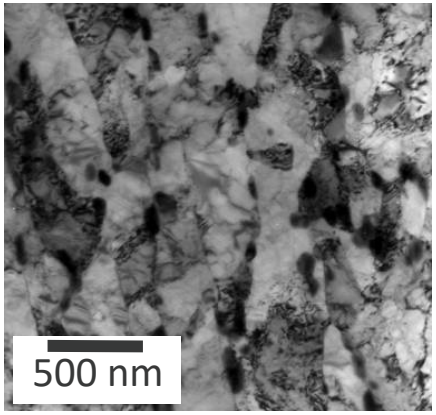

Primary – 100 h

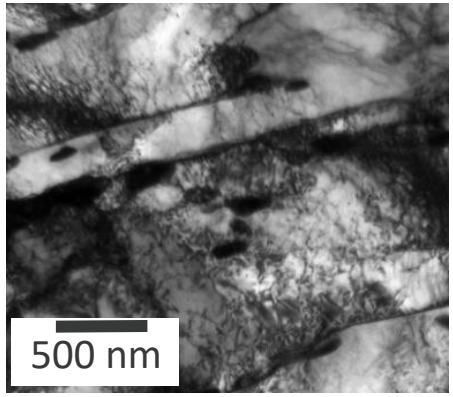

Crept "gage" – 1100 °F

Secondary – 1000 h

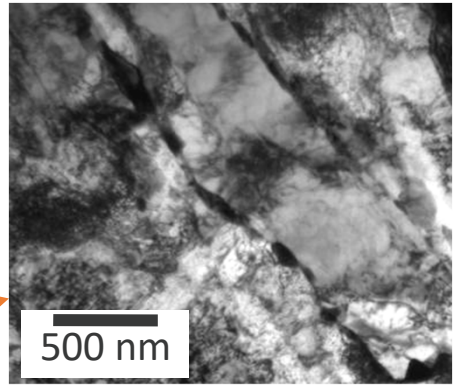

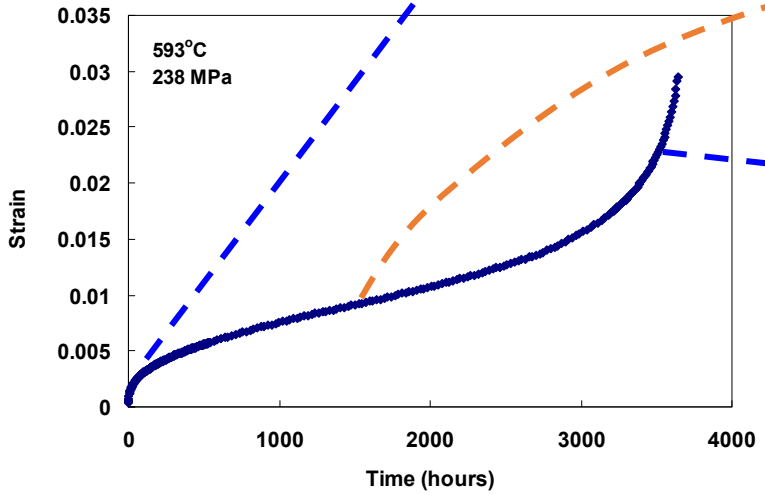

Rupture – 3000 h

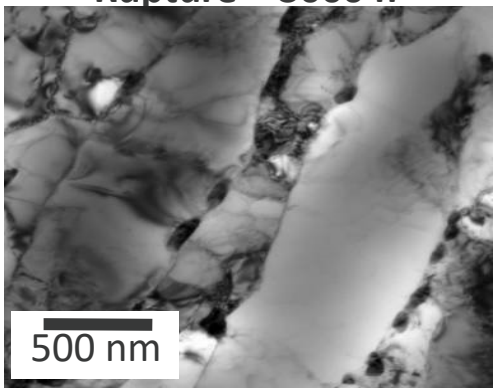

Microstructural Evolution

Subgrain, precipitate, and dislocation structure

- ***Microstructural evolution is inevitable for the high temperature, high stress long service life span FE environment.***
- ***The only option left to extend the life of a material is to slow down this process.***
- ***Modeling and simulations will provide information on stable microstructures which leads to improved cost-effective alloys development for FE systems.***

Haynes 282 Precipitation Kinetics

Baseline alloy

	Al	Co	Cr	Fe	Mo	Ti	Ni	Vol.%
1	1.5	10.0	20.0	1.5	8.5	2.1	Bal	18.86
2	**1.8**	10.0	20.0	1.5	8.5	2.1	Bal	21.08
3	1.5	**11.0**	20.0	1.5	8.5	2.1	Bal	18.91
4	1.5	10.0	**21.0**	1.5	8.5	2.1	Bal	18.97
5	1.5	10.0	20.0	1.5	**9.5**	2.1	Bal	19.05
6	1.5	10.0	20.0	1.5	8.5	**2.5**	Bal	21.62

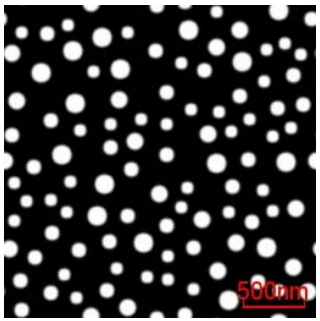

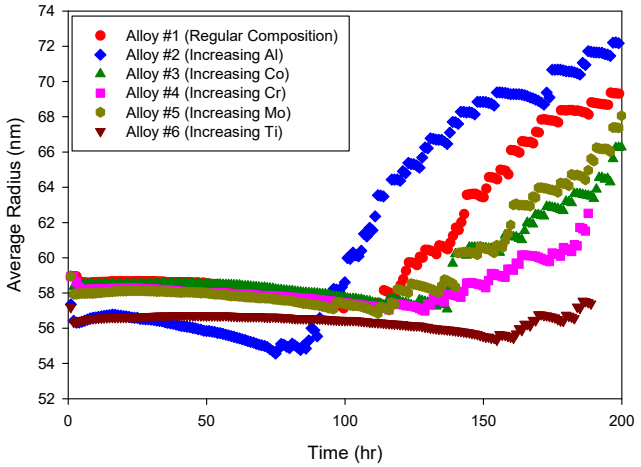

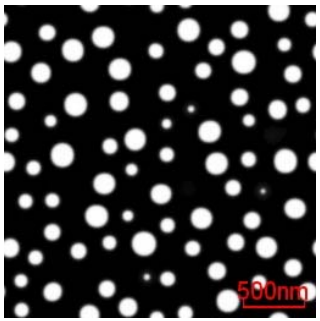

Developed a Virtual Tool for Alloy Chemistry Screening

Precipitation Kinetics Model Validation

Aged at 760°C for 0 to 10,000 hrs , Water Quenched, gamma prime size examined by TEM (20,000 hr sample on-going)

Alloy	Ni	Cr	Co	Mo	Ti	Al	Ti/Al	k
Nominal	Bal	18.5-20.5	9-11	8-9	1.9-2.3	1.38-1.65		
H282-B	Bal	19.22	9.86	8.49	1.94	1.54	1.25	0.38
H282-C	Bal	19.19	9.85	8.50	2.22	1.27	1.75	0.35

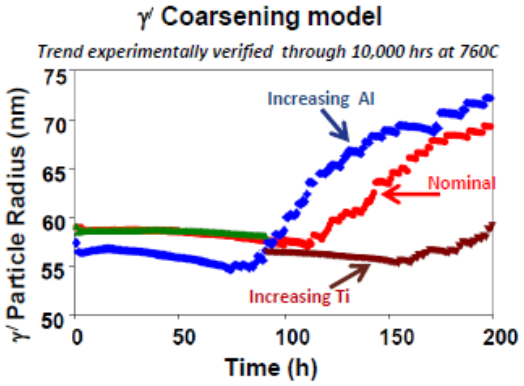

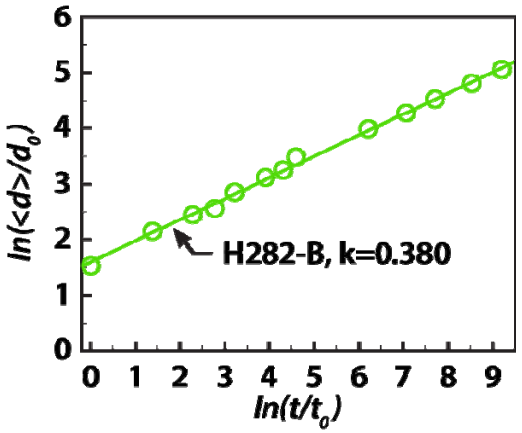

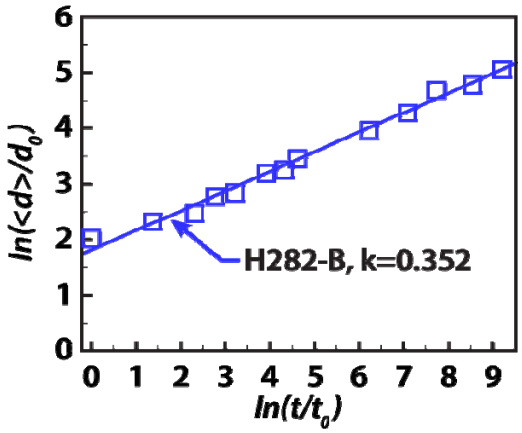

Model predicts higher Ti/Al ratio retards gamma prime coarsening rate
Model experimentally verified

In FY17, NETL plans to optimize the composition, hence, microstructure and performance of another gamma prime strengthened Ni-base alloy of importance to the A-USC program (IN740H)

Remaining Key Technical Gaps for Precipitation Kinetics Modeling

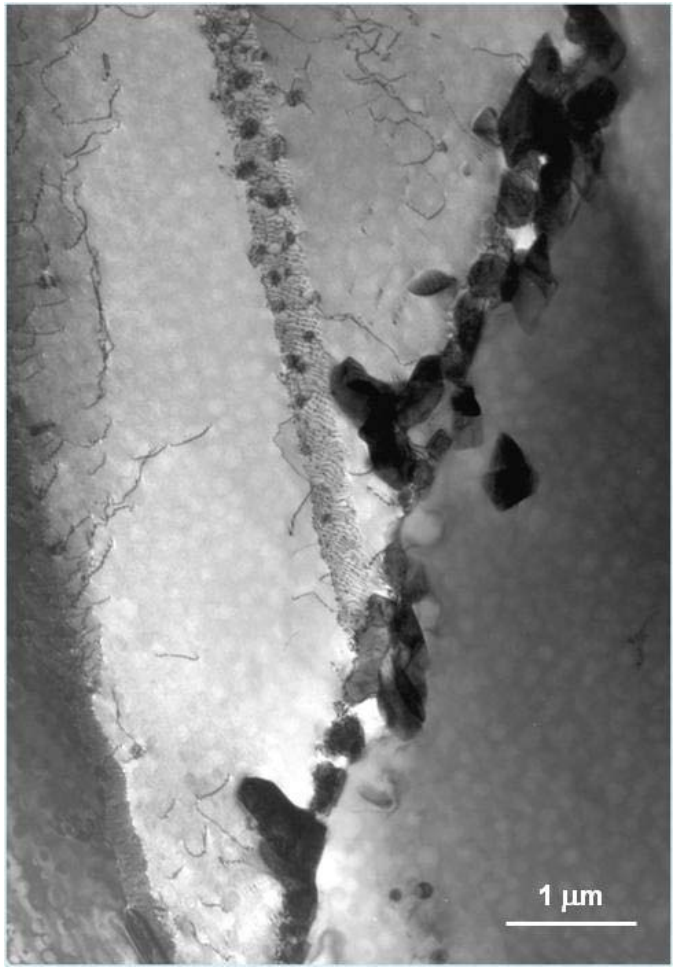

- Our proposed modeling approach is appropriate for early stage coarsening only
- In the late stage when the precipitate grow much bigger, **plastic and viscoplastic deformation usually occur**

This is a common problem in materials science involving precipitates

Bulk Microstructural Stability vs. Surface Attack by Environment

- Microstructural stability inside the **bulk** materials so far …

- **Surface attack** when a material is exposed to a high temperature corrosive environment

Advanced Alloy Development FWP Subtask 3.1 - Computational Investigations & Model Development

Develop modeling toolbox to link material's operating environment to its performance

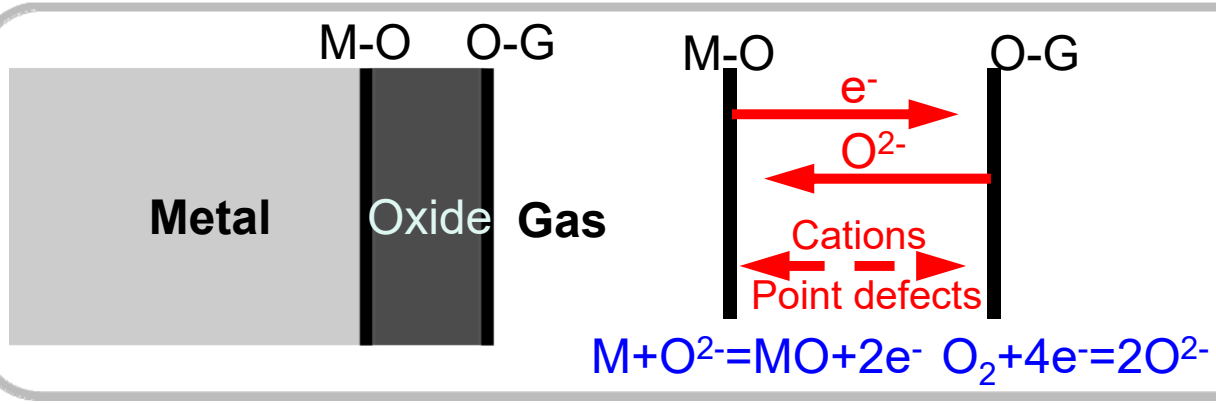

- **Chemical reaction**
- **Mass diffusion**
- **Charge interaction**
- **Microstructural evolution**

Challenges

- High temperature oxidation is a ***complex kinetic process*** consisting of: *chemical reactions*, *mass transport*, *electrostatic interactions and an evolving microstructure.*
- Lack of a physics-based computational model that can predict oxidation kinetics consistently across different time and length scales in realistic applications.

Approach: Develop a physics based phase field model to simulate oxidation scale growth on alloy surfaces. Systematic model development with increasing complexity of process.

Phase-field Method
Governing Equations for Metal Oxidation

NATIONAL ENERGY TECHNOLOGY LABORATORY

Reaction | Diffusion + Electromigration

[X$^-$]: $$\frac{\partial c_1}{\partial t} = K_I \Lambda_\zeta (Q\tilde{c}_2 - \tilde{c}_1) - K_{II}\Lambda_\eta \tilde{c}_1 + \nabla\cdot(\tilde{D}_1 \nabla \tilde{c}_1) - \frac{e}{k_B T}\nabla\cdot(D_1 c_1 z_1 \mathbf{E})$$

[e$^-$]: $$\frac{\partial c_2}{\partial t} = -K_I \Lambda_\zeta (Q\tilde{c}_2 - \tilde{c}_1) + K_{II}\Lambda_\eta \tilde{c}_1 + \nabla\cdot(\tilde{D}_2 \nabla \tilde{c}_2) - \frac{e}{k_B T}\nabla\cdot(D_2 c_2 z_2 \mathbf{E})$$

[c$^+$]: $$\frac{\partial c_3}{\partial t} = \nabla\cdot(D_3 \nabla c_3) - \frac{e}{k_B T}\nabla\cdot(D_3 c_3 z_3 \mathbf{E})$$

[M]: $$\frac{\partial \eta}{\partial t} = -K_V K_{II}\Lambda_\eta \tilde{c}_1 + M_\eta \nabla^2\left(\partial f / \partial \eta - \beta \nabla^2 \eta\right)$$

The electric field, satisfying Poisson's equation, is solved by **an efficient numerical scheme** for *arbitrary* **dielectric heterogeneity**

$$\nabla\cdot[\varepsilon(\mathbf{r})\nabla\varphi(\mathbf{r})] + \rho_f(\mathbf{r}) = 0$$

Cheng & Wen, PRE 2015

Advanced Alloy Development FWP Subtask 3.1 - Computational Investigations & Model Development

Major accomplishments

★ Developed *physics-based* phase field model to fully describe oxide scale growth:

- ✓ General formulation of corrosion kinetics in oxidation & sulfidation conditions. ***Uses realistic free energies and kinetic data resulting in quantitative predictions with minimal approximations.*** (*Simul. Mater Sci. Engr.*, **20** (2012) 034013).
- ✓ Extended ***novel multi-scale simulation*** scheme to account for coupling of transport of ionic species across scales → ***seamlessly covers a wide range of length- and time-scales,*** and couples interfacial reaction and ionic transport with moving boundary ***without a priori assumptions.*** (*J. Phys Chem C*, **118** (2014) 1269-1284).
- ✓ Developed ***efficient numerical algorithm*** to solve charge interaction problem with arbitrary heterogeneity in electric properties. (*J. Phys. Chem Letters*, **5** (2014) 2289-2294; *Physical Review E*, **91** (2015) 05307)

★ Lays ground work for future model development in more complex alloys & environments.

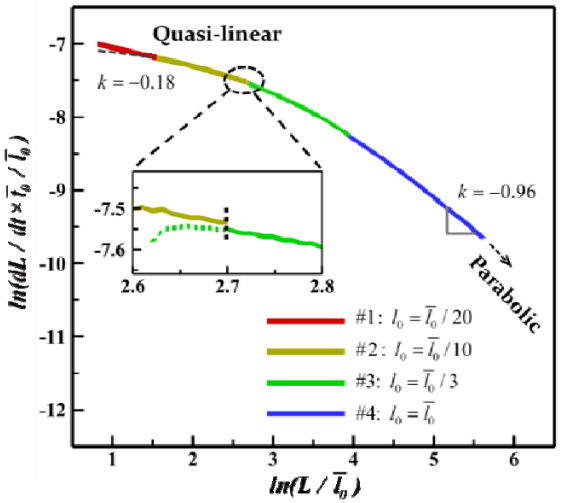

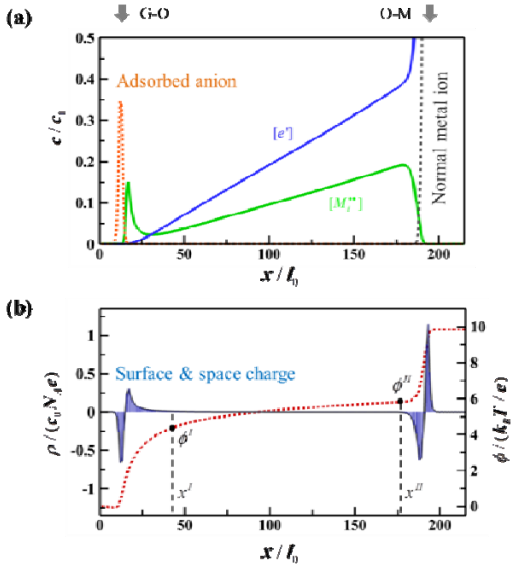

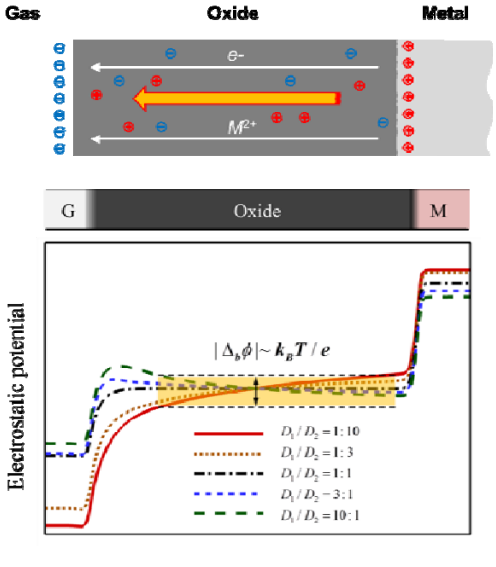

Adopted by others to predict the kinetics of V_2O_3 hot-corrosion on TBC's: A. Abdulhamid et al., *Comp. Mater. Sci.*, 99 (2015) 105-116)

Subtask 3.1: Computational Investigations & Model Development

Past efforts in this subtask delivered physics-based modeling capabilities on

External Oxidation

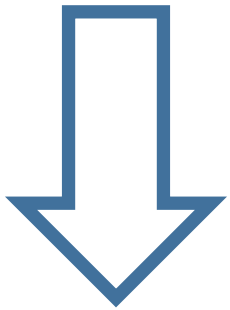

On-going efforts focus on modeling

Internal Oxidation

Modeling Internal Oxidation

Why we care?

- Oxidation usually starts with internal selective oxidation of certain solute elements
- Transition from internal to external oxidation is the basis for alloy design regarding oxidation resistance.

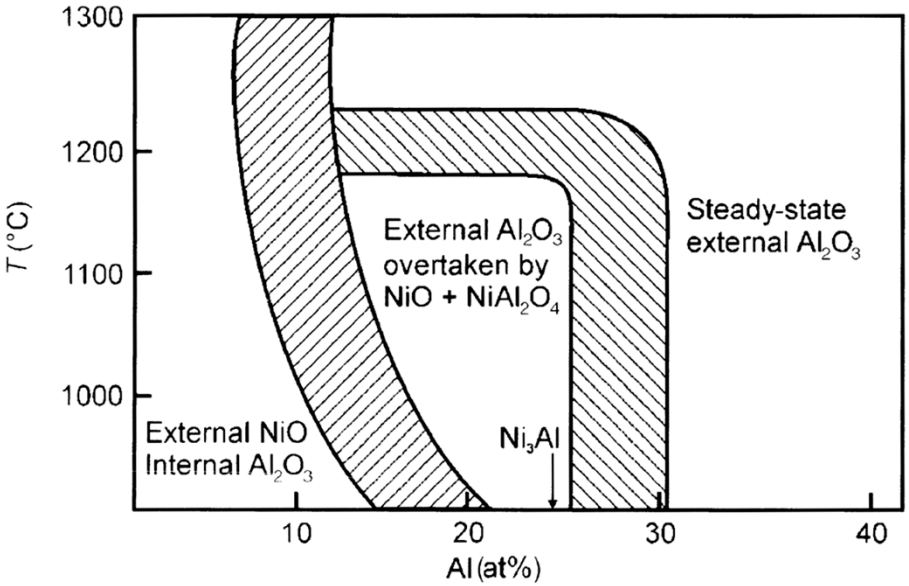

Oxidation Map:
Compositional effects on the oxidation of Ni-Al alloys (N. Birks, G. Meier, F. Pettit, 2006)

Theoretical Understanding on Internal Oxidation

Wagner theory for a binary system with 1D assumption – **Oversimplification!**

Remains an **open problem** especially in consideration of the complex microstructure involved in internal oxidations

Wagner's theory on the transition from internal to external oxidation

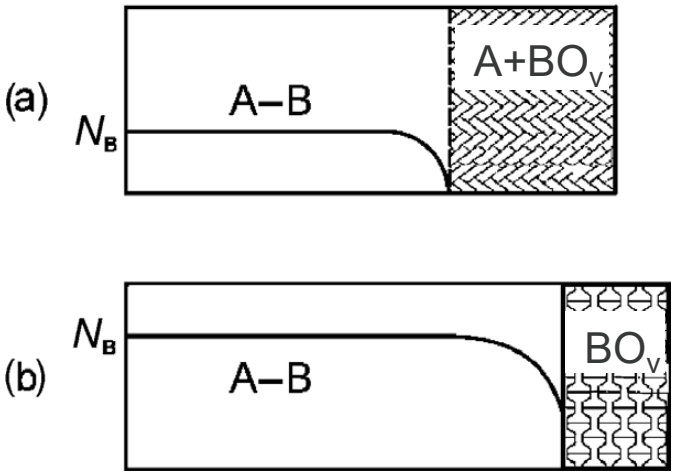

Schematic: transition from internal to external oxidation of solute B.
(a) internal oxidation,
(b) external oxidation with higher CB

(after N. Birks, G. Meier, F. Pettit, 2006)

Transition criterion (C. Wagner 1959):

$$N_B^{(O)} > \left[\frac{\pi f^*}{2\nu} \frac{V_m}{V_{ox}} \frac{D_O N_O^{(S)}}{D_B} \right]^{1/2}$$

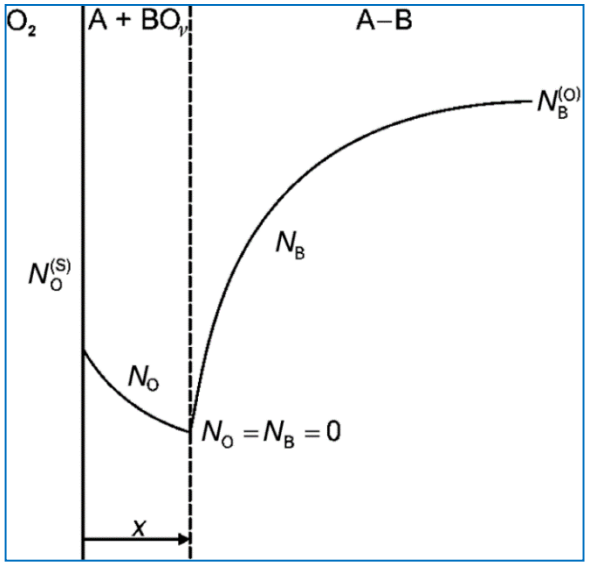

Schematic: Concentration profiles for internal oxidation of A-B (Birks, Meier, Pettit, 2006)

Wagner's theory on the transition from internal to external oxidation

Transition criterion (C. Wagner 1959):

$$N_B^{(O)} > \left[\frac{\pi f^*}{2\nu} \frac{V_m}{V_{ox}} \frac{D_O N_O^{(S)}}{D_B} \right]^{1/2}$$

$f^* = 0.3$ (for Ag-In system) (R. A. Rapp, 1961)

$f^* \sim 0.5$ (for Fe-Si system) (W. Zhao, Y. Kang, J. Orozco, B. Gleeson, 2015)

There is no universal/general f^* even just for binary systems!

No Predication Capability!

Different Internal Oxidation Microstructures

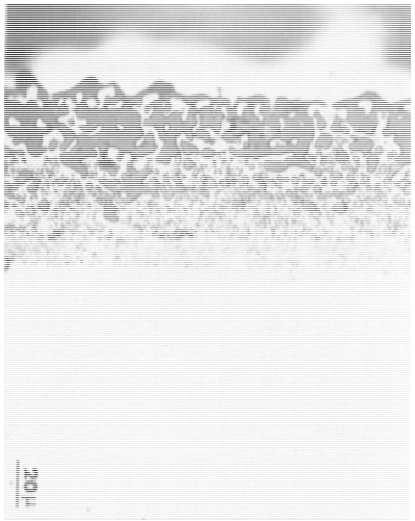

Co-8.99%Ti oxidized at 900˚C for 528h, (J. Megusar; G. Meier, 1976)

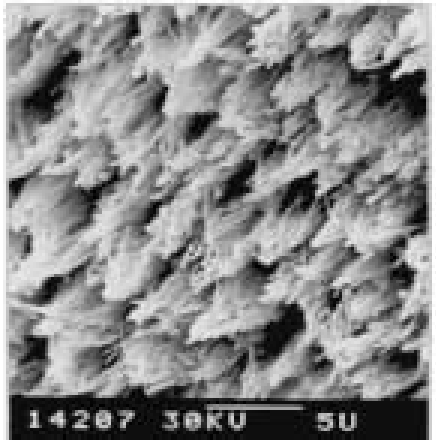

Ni-8.67Al oxidized at 1000˚C (after deep etching) (A. M.-Villafane, F. Stott, J. C.-Nava, G. Wood, 2002)

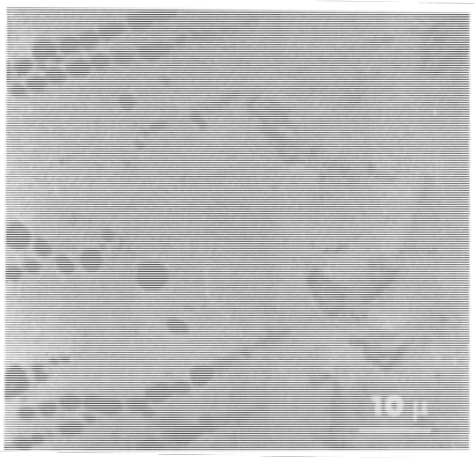

TiO_2 needles in Co-3.7Ti alloys after reaction front passed. (J. Megusar and G. Meier, 1976)

No universal critical volume fraction of internal oxide for the transition from internal to external oxidation

Internal Oxidation Morphology

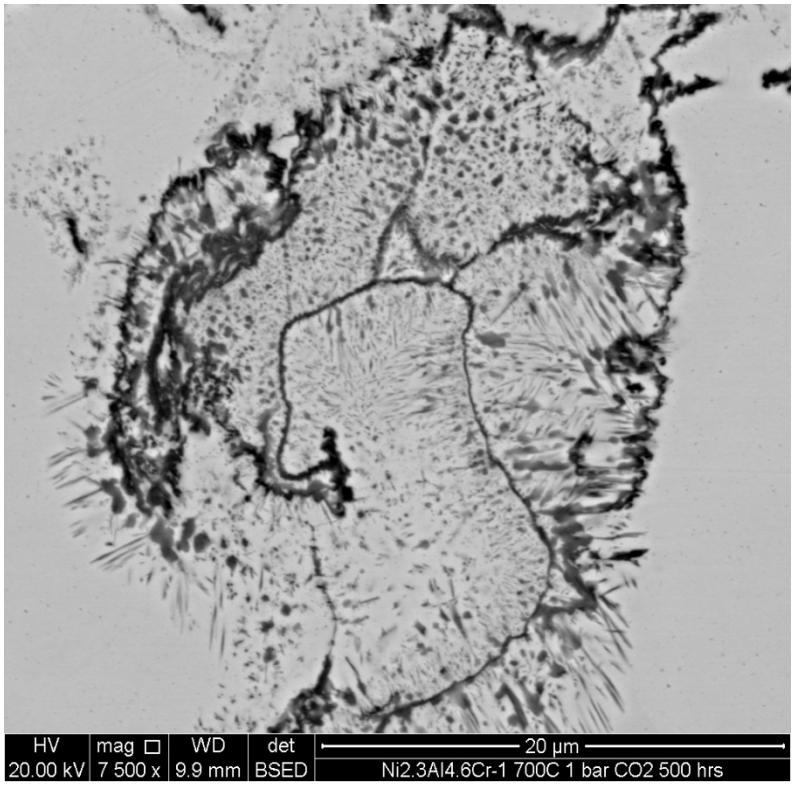

Internal oxidation in Ni-2.3Al-4.6Cr after 500 h in 1 bar CO_2 at 700°C (Chromia is typically more spherical & Alumina is more lathe-like)

Courtesy of Gordon R. Holcomb

A complex concurrent diffusion, nucleation, growth, and coarsening problem

- Diffusion coupled nucleation has to be implemented
- Anisotropic growth has to be considered due to drastically different interfacial energies
- Growth induced local stress has to be considered, *which is exactly the same problem as mentioned before for late stage precipitate growth modeling*

Phase-Field Modeling of Internal Oxidation and Its Transition to External Oxide?

NATIONAL ENERGY TECHNOLOGY LABORATORY

- Phase-Field Method appears to be well suited for modeling the complex morphological evolution during the internal to external oxidation transition process! At least phase-field has the potential
- But there are a few challenges …

Large Deformation Associated with Oxide Growth

Table 5.1 *Oxide–metal-volume ratios of some common metals*

Oxide	Oxide–metal-volume ratio
K_2O	0.45
MgO	0.81
Na_2O	0.97
Al_2O_3	1.28
ThO_2	1.30
ZrO_2	1.56
Cu_2O	1.64
NiO	1.65
FeO (on α-Fe)	1.68
TiO_2	1.70–1.78
CoO	1.86
Cr_2O_3	2.07
Fe_3O_4 (on α-Fe)	2.10
Fe_2O_3 (on α-Fe)	2.14
Ta_2O_5	2.50
Nb_2O_5	2.68
V_2O_5	3.19
WO_3	3.30

(Hancock and Hurst, 1974)

- Plastic & viscoplastic deformation during oxide growth is usually unavoidable
- Plastic and viscoplastic deformation will relieve local stress and therefor influence the growth kinetics and the morphology of oxide.

Need to Develop a Plastic and Viscoplastic Deformation Modeling Capability!

Phase field models involving plasticity - classical plasticity theories

$$\varepsilon = \varepsilon^{el} + \varepsilon^{0} + \varepsilon^{pl}$$

Convex dissipation potential :
(Lemaitre and Chaboche, 1990)

$$\Omega(\sigma, X, R) = \int_V \tilde{\Omega}(\sigma, X, R)\, dV$$

- The postulated convex dissipation potential, if explicitly given, does **not** have a clear connection to the free energy assumed in the phase-field formulation
- Plastic flow is loosely coupled with microstructure evolution through total strain.

Example:

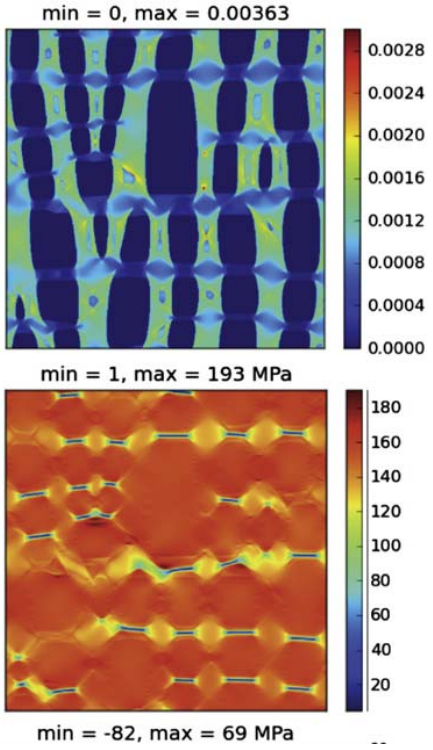

(Cottura et al. *J. Mech. Phys. Solids*, 2012)

Phase field modeling of plasticity

In any phase-field models, a free energy functional for the whole material system is defined

The microstructural evolution is governed by kinetic equations derived from the free energy functional through variational principles.

Why can't plastic deformation be derived from the same free energy functional for the sake of self-consistency?

Phase field modeling of plasticity

Continuum (coarse-grain) level

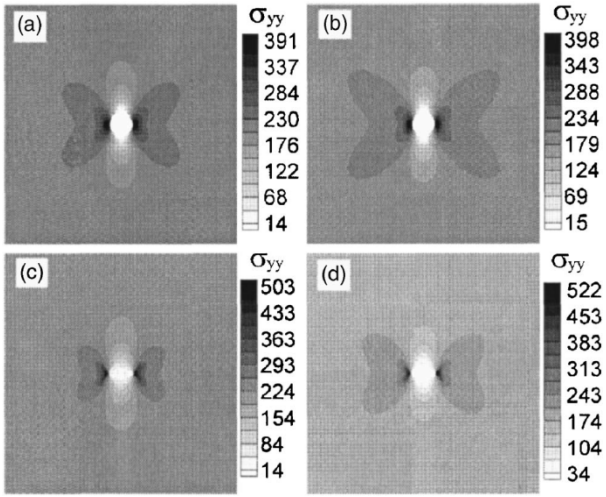

Guo, Shi, and Ma, *Appl. Phys. Lett.*, 2005, reiterated/revised by Yamanaka 2008, Yeddu 2012

There have been attempts along this line with the first by Prof. Shi's group from Hong Kong.

- Only elastic-perfectly-plastic constitutive relations were considered, i.e. without any strain hardening.
- **Plastic strain is solved by minimizing shear strain energy alone**.

Can the plastic strain be solved by minimizing the total free energy functional instead?

Simulation results vs analytical solutions

1. Elasto-plastic inclusion problem: elastic/perfectly-plastic matrix

Radial and tangential stress distribution

$$\begin{cases} \sigma_r = \sigma_\theta = \sigma_I, \ 0 \le r \le a; \\ \sigma_r = \sigma_\theta - \sigma_Y^0 = \sigma_I + 2\sigma_Y^0 \ln\left(\dfrac{r}{a}\right), a \le r \le r_p; \\ \sigma_r = -2\sigma_\theta = -\dfrac{2\sigma_Y^0}{3}\left(\dfrac{r_p}{r}\right)^3, \ r_p \le r < \infty, \end{cases}$$

Size of plastic zone:

$$r_p = \left(\frac{6\mu\alpha\varepsilon}{\sigma_Y^0}\right)^{1/3} a$$

Analytical solution by (Lee, Earmme, Aaronson, and Russell, *Metal. Trans. A* 1980)

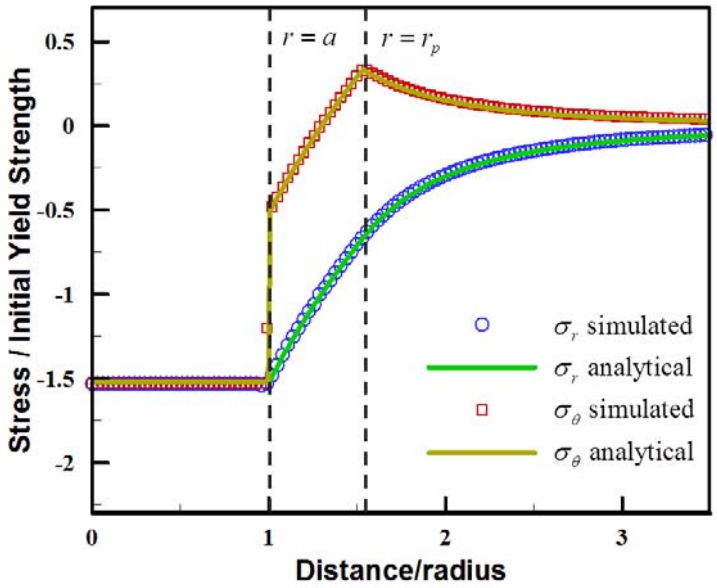

Simulated distributions of stress components in radius direction as compared to analytical solution; matrix being elasto-perfectly-plastic

Simulation results vs analytical solutions

2. Elasto-plastic inclusion problem: linear elastic-plastic matrix

Radial and tangential stress distribution

$$\begin{cases} \sigma_r = \sigma_\theta = \sigma_I, \ 0 \le r \le a; \\ \sigma_r = \dfrac{2\sigma_Y^0}{3}\left[3\ln\left(\dfrac{r}{r_p}\right) - 2\phi(1-\nu)\left(\dfrac{r_p}{r}\right)^3 - 1\right], \ a \le r \le r_p; \\ \sigma_\theta = \dfrac{2\sigma_Y^0}{3}\left[3\ln\left(\dfrac{r}{r_p}\right) + \phi(1-\nu)\left(\dfrac{r_p}{r}\right)^3 + \dfrac{1}{2}\right], \ a \le r \le r_p; \\ \sigma_r = -2\sigma_\theta = -\dfrac{2\sigma_Y^0}{3}\left(\dfrac{r_p}{r}\right)^3, \ r_p \le r < \infty, \end{cases}$$

Size of plastic zone:

$$r_p = \left(\frac{6\mu\alpha\varepsilon}{\sigma_Y^0}\right)^{1/3} a$$

Analytical solution by (Earmme, Johnson, Lee, *Metal. Trans. A* 1981)

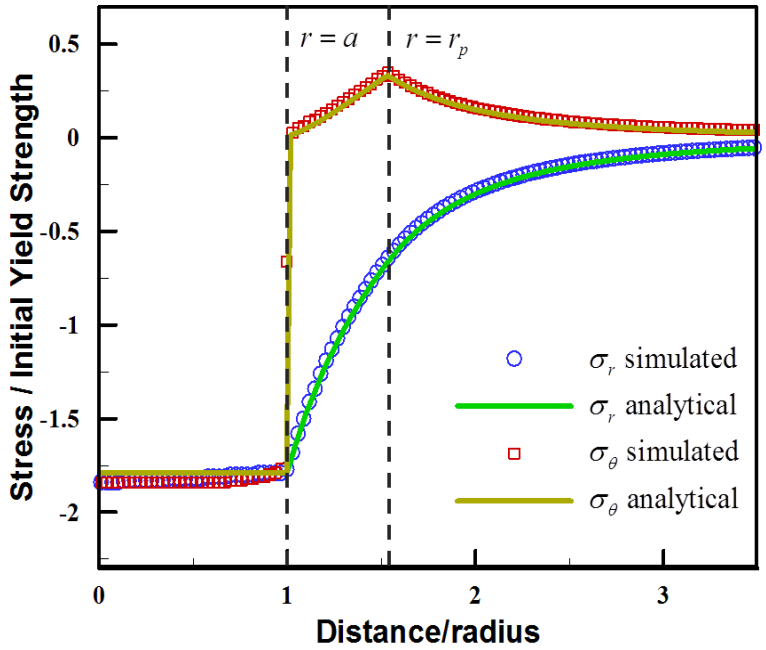

Simulated distributions of stress components in radius direction as compared to analytical solution; matrix being elasto-plastic with linear hardening

Simulation results vs analytical solutions

3. Elasto-plastic inclusion problem: elastic-plastic matrix with power-law hardening

Analytical solution NOT available!

Phase-field simulation compared to numerical solutions
(Earmme, Johnson, Lee, *Metal. Trans. A* 1981)

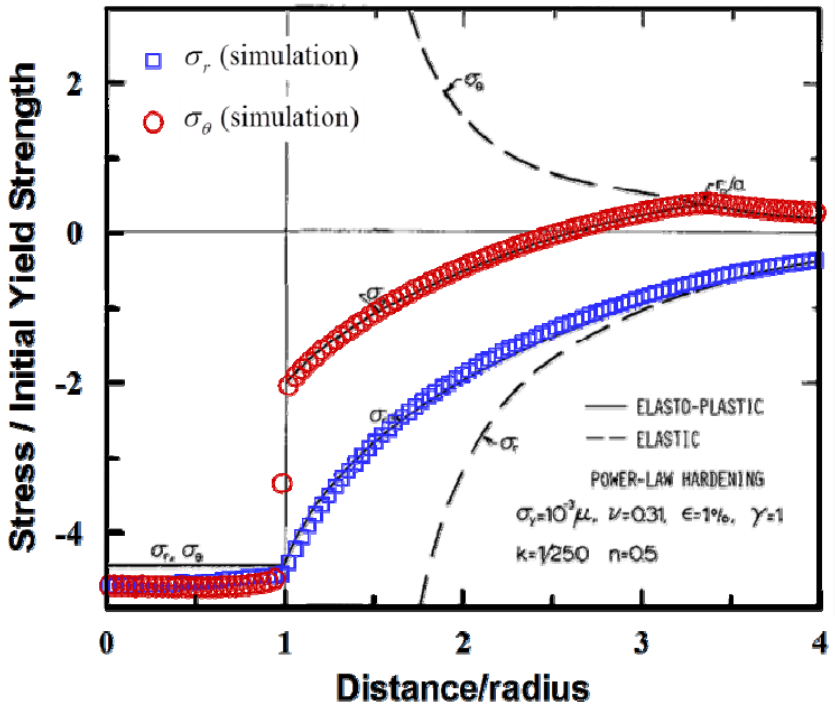

Simulated distributions of stress components in radius direction as compared to analytical solution; matrix being elasto-plastic with power-law hardening

NATIONAL ENERGY TECHNOLOGY LABORATORY

4. Elasto-plastic inclusion problem: elastic/perfectly-plastic matrix with a free surface

Radial and tangential stress distribution

$$\begin{cases} \sigma_r = \sigma_\theta = \sigma_I, \ 0 \le r \le a; \\ \sigma_r = \sigma_\theta - \sigma_Y^0 = \sigma_I + 2\sigma_Y^0 \ln\left(\dfrac{r}{a}\right), \ a \le r \le r_p; \\ \sigma_r = 4\mu\alpha\varepsilon a^3\left(\dfrac{1}{b^3} - \dfrac{1}{r^3}\right), \ r_p \le r \le b; \\ \sigma_\theta = 4\mu\alpha\varepsilon a^3\left(\dfrac{1}{b^3} + \dfrac{1}{2r^3}\right), \ r_p \le r \le b, \end{cases}$$

Analytical solution developed in this work

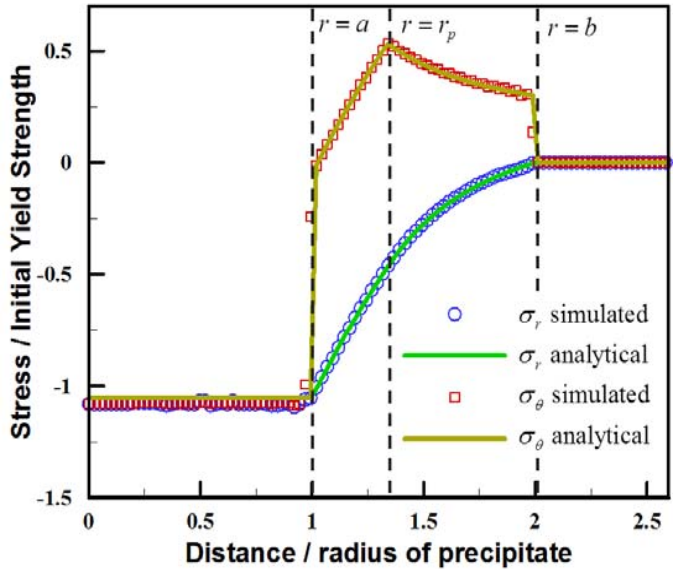

Simulated distributions of stress components in radius direction as compared to analytical solution; matrix being elasto-perfectly-plastic with a free surface

Application 1: Modeling the incoherent interfaces

Simulated precipitate shape evolution toward equilibrium

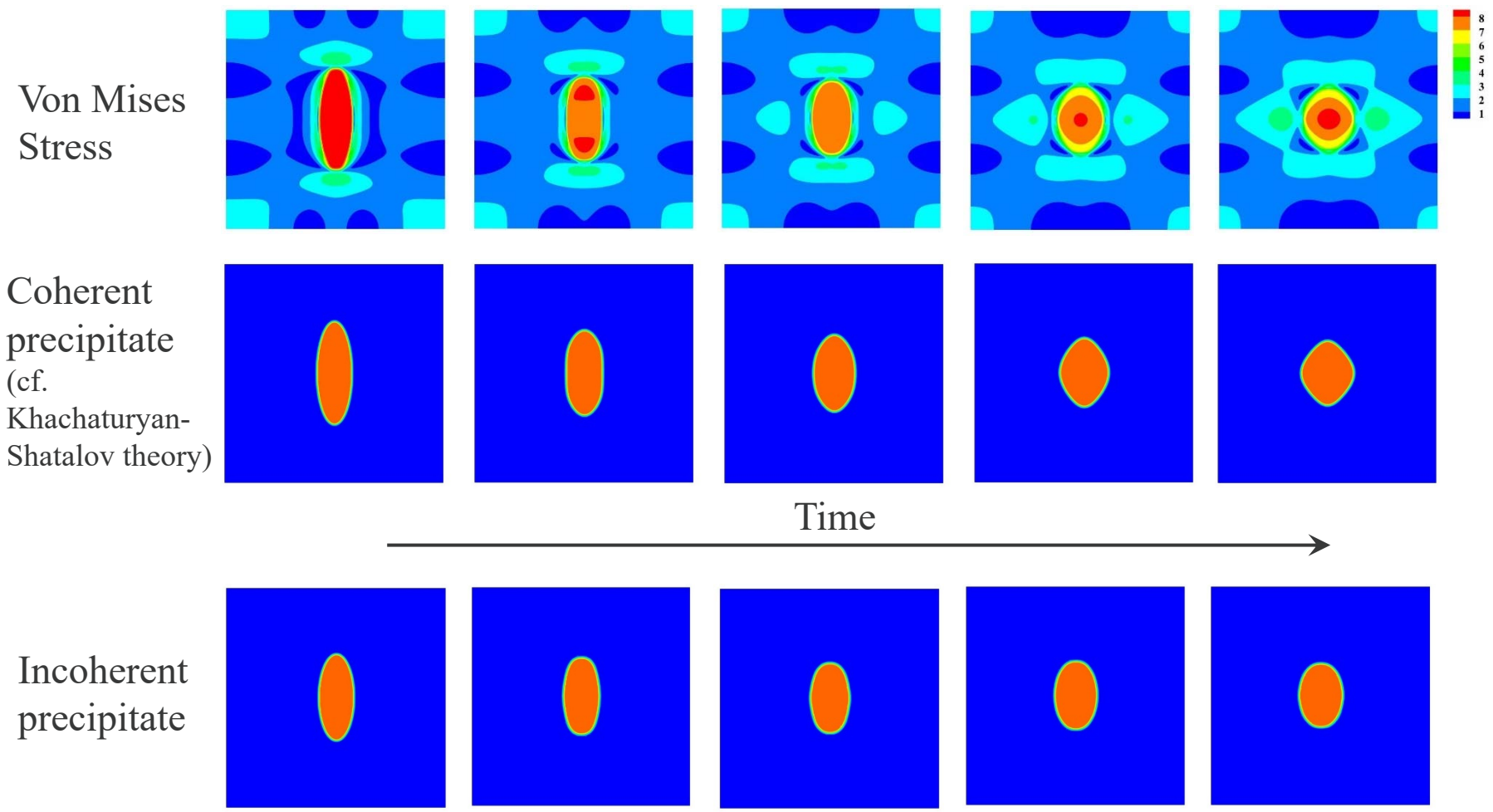

Application 2:
Modeling Spallation of Oxide(s)

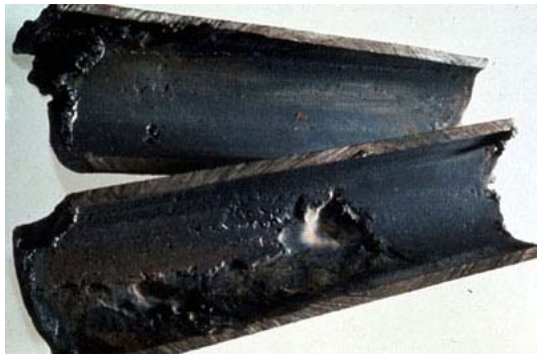

Boiler Tubing

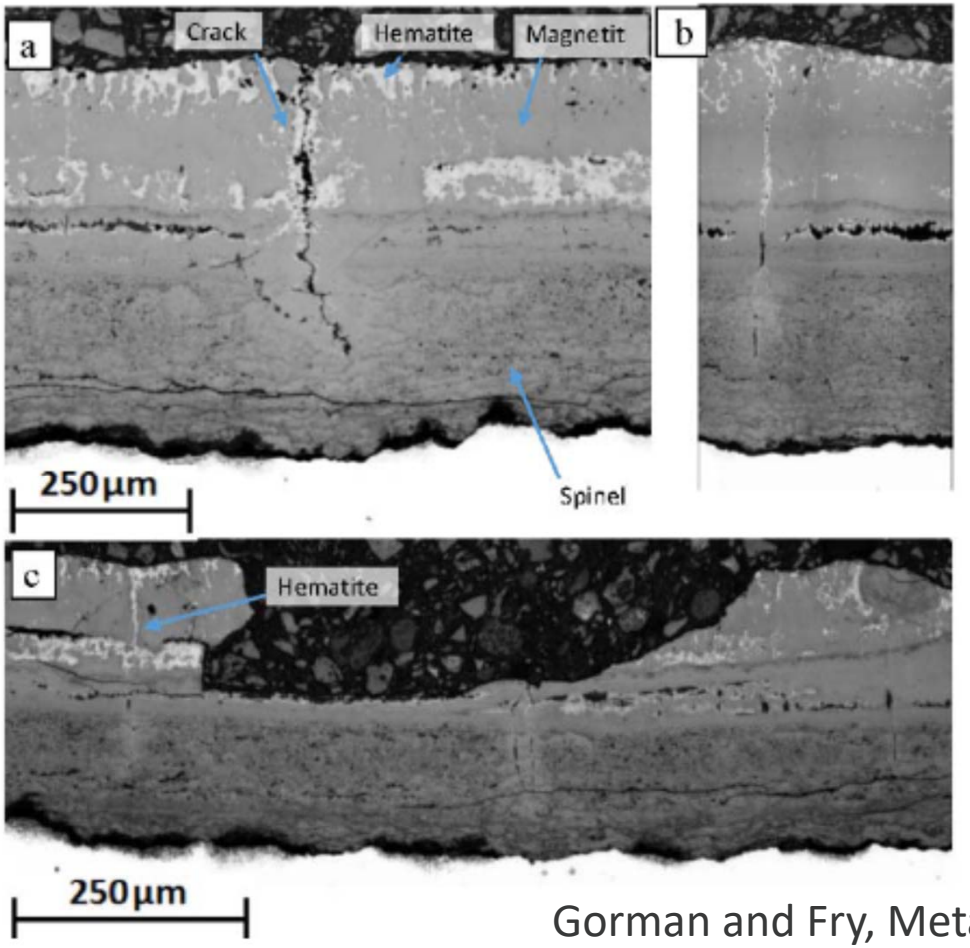

Gorman and Fry, Metals, 2016

Micrographs of T91 Ferritic exposed in plant for 91 kh in the temperature range 500-650C at elevated pressure showing (a,b) through thickness cracking and © region of spalled oxide.

Summary

- Proposed a new approach to formulate elasto-viscoplasticity within a consistent phase-field framework as part of the ongoing efforts towards physics-based internal oxidation modeling
- Model has the potential to simulate other important processes involved in oxidation, such as incoherent interfaces and spallation